Semi-analytical investigations of R-curve behavior in ferroelectric materials considering different scales

Roman Gellmann[1,a], Andreas Ricoeur[1,b]

[1] Institute of Mechanics, University of Kassel, Moenchebergstr. 7, 34125 Kassel, Germany

[a] gellmann@uni-kassel.de, [b] andreas.ricoeur@uni-kassel.de

Keywords: Ferroelectrics, small scale switching, fracture toughness, Coulomb tractions.

Abstract. In the present work we study the effective fracture toughness of ferroelectrics by taking the mesoscopic as well as the macroscopic level into account. On the macroscopic scale we apply an extended theory of stresses at interfaces in dielectric solids [1,2]. Further, on the mesoscopic scale, nonlinear effects are introduced by applying the small scale switching approximation, i.e. the effects are limited to a small region around the crack tip. Finally, we discuss the effective fracture toughness and crack resistance curves for different loading and poling conditions. The analysis is done considering the full anisotropy and electromechanical coupling of the material by using piezoelectric weight functions [3]. In contrast to previous approaches, the presented model also takes the inverse switching (180 degree) into account yielding a contribution to the electric displacement intensity factor.

Introduction

Due to the brittleness of ferroelectric materials fracture mechanical approaches are playing an essential role in the modern research. The strength of these materials is significantly determined by nonlinear ferroic effects arising on the mesoscopic scale. In ferroelectrics, the most important toughening mechanism is the switching of polarization (domain switching) in the vicinity of crack-tips. Following a common term in elasto-plastic-fracture mechanics this is called “small scale switching”, a topic which has been studied by some researchers during the past three decades [4-7]. Particularly during the past few years it came out from theoretical approaches that another crack closing effect, which is based on macroscopic considerations, plays a non-negligible role too [8,1]. This one is due to the electrostatics of interfaces exposed to electric fields effecting crack surface tractions. Besides theoretical work, a number of experiments has been carried out [9-12] with results significantly dependent on the loading conditions, poling direction and orientation of the crack with respect to the poling axis. The influence of electric fields on fracture toughness and crack propagation has been investigated with partly inconsistent results. The reason behind this could be due to a complicated fracture criterion which is still not yet completely understood. Thus, essential influences on the fracture toughness might be unknown and thus disregarded in the experiments.

The mechanics of ferroelectric materials is based on the combination of the microscopic switching behavior and the reversible linear behavior [13-21]. The coupling between the micromechanical model for polarization switching and effects on the macroscopic scale [8,1] with respect to crack tip shielding is presented in this work to gain a deeper understanding of the effective fracture toughness and crack growth resistance (R-curve) behavior in ferroelectric materials.

The knowledge of R-curves is essential to examine processes of slow stable crack growth and to determine the bifurcation to unstable fracture. Toughness variation and R-curves within state of the art models are mostly calculated based on ferroelectric inclusions in a linear elastic matrix,

neglecting the anisotropy and field coupling of ferroelectric materials. These calculations have been made for simple fully permeable crack face boundary conditions and do not exhibit any R-curves. In general, the state of the art models are using a simple switching criterion according to Hwang et al. [22].

In contrast to previous works our semi-analytical calculations are based on a model which accounts for an extended switching criterion, piezoelectric crack weight functions and the full anisotropy of ferroelectric materials. Also, the contribution from 180°-switching (inverse switching) is incorporated. On the macrosopic scale, crack face boundary conditions are chosen closely to reality, incorporating electrostatic crack face tractions and charges. Thus, effects on macro- and microscale are coupled, requiring an iterative numerical solution procedure. The modeled specimens are exposed to critical mode-I and combined mode-I and mode-IV loadings, poling is perpendicular or parallel to the crack faces.

Theoretical Framework

The strength of ferroelectric materials, in terms of the critical stress intensity factors, is significantly determined by nonlinear ferroic effects arising on the microscopic scale. These effects are modeled by decomposing the strain ε_{ij} and electric displacement D_i additively into a linear piezoelectric part denoted with a superscript *rev* and a remanent strain $\Delta\varepsilon_{ij}$ and remanent polarization ΔP_i emerging due to polarization switching phenomena. The macroscopic constitutive law in a representative domain (RVE) is given by

$$\varepsilon_{ij} - \Delta\varepsilon_{ij} = S_{ijkl}\sigma_{kl} + g_{kij}(D_k - \Delta P_k) \tag{1}$$

$$E_i = -g_{ikl}\sigma_{kl} + \beta_{ik}(D_k - \Delta P_k) \tag{2}$$

Here, ε_{ij}, σ_{ij}, E_i and D_k are respectively the components of the total strain, local stress tensor, electric field and electric displacement vector. S_{ijkl}, g_{ikl} and β_{ik} are the reduced elastic compliances, piezoelectric constants and the dielectric impermeability, respectively. The stresses σ_{ij} and electric displacement D_k are expressed in terms of the near-field solution. This means that the problem under consideration is in general an arbitrary crack. The crack tip loading K_L^{tip} is given by the superposition of the applied loads K_L^{app} and the loads induced due to polarization switching $\Delta K_L(K_L^{app})$:

$$K_L^{tip} = K_L^{app} + \Delta K_L(K_L^{app}), \qquad \text{where} \qquad \Delta K_L = \int_{(A)} h_{LN,j}(r,\varphi)\,\Delta\Sigma_{Nj}\,dA. \tag{3}$$

The subscript L like all capital indices ranges from 1 to 4 and represents the three mechanical and the dielectric crack opening modes. It is worth noting, that by contrast to the state-of-the-art, the calculations performed in this work are done using the full anisotropy of the material and piezoelectric weight functions h_{LN} that have been derived in [3]. $\Delta\Sigma_{Nj}$ is the irreversible, i.e. remanent part of the generalized stress tensor which is assumed to be homogeneous within the process zones. The global fracture criterion can be written as $K_L^{app} \geq K_{LC}$, where the subscript "C" denotes the material-specific fracture toughness required for critical crack growth. It is therefore obvious that the fracture toughness is strongly modified by polarization switching phenomena. On

the other hand, in a recent work [1] it was shown, that for a more general crack model in piezoelectric materials which considers also the macroscopic electrostatic crack surface tractions σ_{22}^{C}, the effective stress intensity factor K_L^{app} is significantly modified. In the present work we calculate the relevant contributions to the effective fracture toughness coupling the macroscopic and microscopic scales and analyze the dependence on the external loads and the poling direction.

Within each domain (RVE) the polarization P is assumed to switch as soon as mechanical and electrical energy reduction exceeds a critical energy barrier w_{crit}. The switching is interpreted as the rotation of the polarization vector around the out-of-plane axis, see Figure 1.

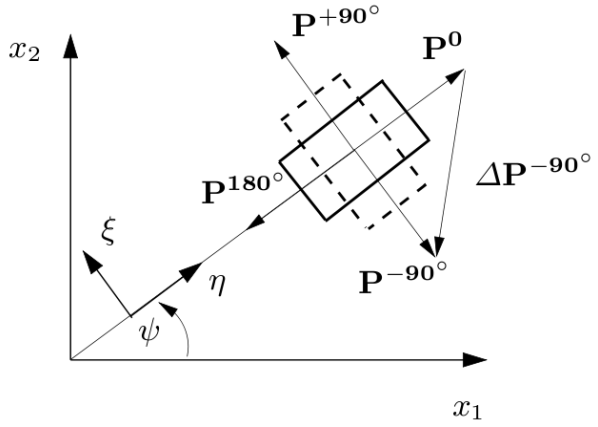

Fig. 1. Three possible switching events of a tetragonal crystal unit cell in a plane.

The variant of the switching $\pm 90^\circ$ or 180° is determined by the switching criterion, such as

$$\sigma_{ij}(\varepsilon_{ij}^{rev} + \Delta\varepsilon_{ij}) + E_i(D_i^{rev} + \Delta P_i) \geq w_{crit}, \quad \text{where} \quad w_{crit}^{\pm 90^\circ} = \sqrt{2}E_C P^0,\ w_{crit}^{180^\circ} = 2E_C P^0. \quad (4)$$

That is, the mechanical stresses and the electric field components are assumed to be known and are not modified by the switching events. The components of the remanent strain $\Delta\varepsilon_{ij}$ and remanent polarization ΔP_i within the local coordinate system (η, ξ) were introduced in [2]:

$$\Delta\bar{\varepsilon}_{ij}(\pm 90^\circ) = \varepsilon_D \begin{pmatrix} 1 & 0 \\ 0 & -1 \end{pmatrix},\ \Delta\bar{P}_k^{+90^\circ} = P^0 \begin{pmatrix} -1 \\ 1 \end{pmatrix},\ \Delta\bar{P}_k^{-90^\circ} = P^0 \begin{pmatrix} -1 \\ -1 \end{pmatrix},\ \Delta\bar{P}_k^{180^\circ} = P^0 \begin{pmatrix} -2 \\ 0 \end{pmatrix}. \quad (5)$$

Note, there is no partial switching allowed. Once the polarization switches, the irreversible strain is locked and cannot be reverse-switched.

Results

We consider two important poling directions: poling perpendicular (x_2-direction) and parallel (x_1-direction) to the crack faces. Further, the intrinsic fracture toughness K_{IC}^{tip} is assumed to be $2\,MPa\sqrt{m}$ which is a typical value for the ferroelectric materials. The crack length is $5\,mm$. It should be noted that all calculations were iterated until Eq. (3) and the electrostatic boundary

conditions at the crack faces were satisfied. The obtained R-curves are plotted in Figures 2 and 3. Here, solid curves represent the impermeable crack model and dashed curves stand for the semi-permeable crack model including crack surface tractions, see [1].

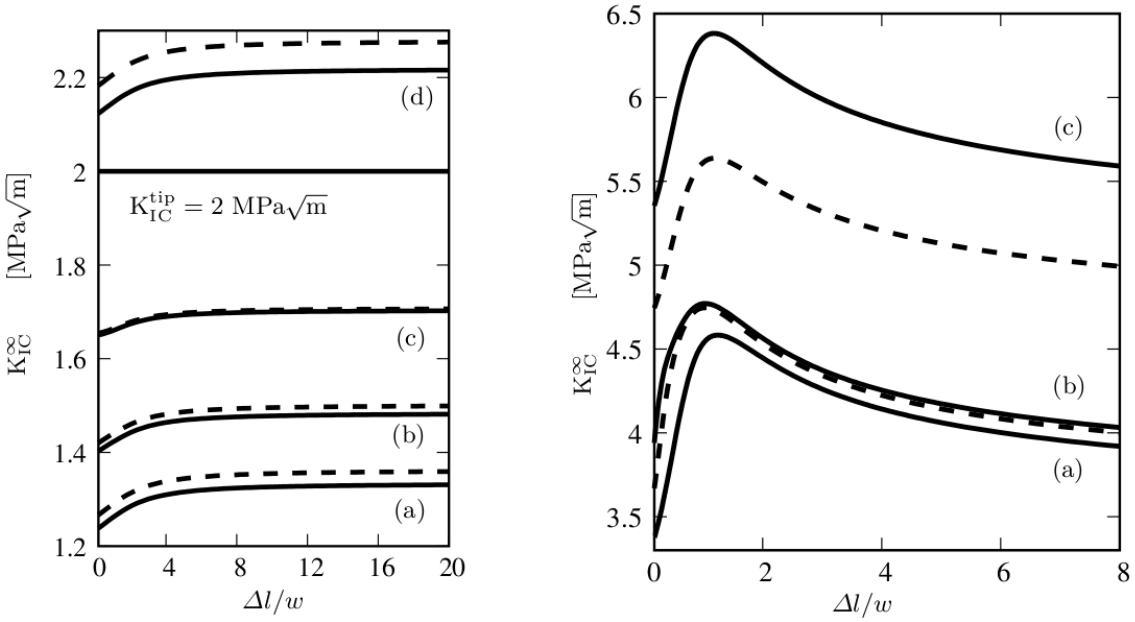

Fig. 2. R-curves for mode-I stress intensity factor of PZT-5H with poling (left) perpendicular and (right) parallel to the crack faces and combined electromechanical loading. The electrical loads are: (a) $K_{IV}^{\infty} = 0 \cdot K_{IV}^{C}$, (b) $K_{IV}^{\infty} = 0.1 \cdot K_{IV}^{C}$ (left), $K_{IV}^{\infty} = 0.3 \cdot K_{IV}^{C}$ (right), (c) $K_{IV}^{\infty} = 0.3 \cdot K_{IV}^{C}$ (left), $K_{IV}^{\infty} = 0.6 \cdot K_{IV}^{C}$ (right) and (d) $K_{IV}^{\infty} = 1.25 \cdot K_{IV}^{C}$.

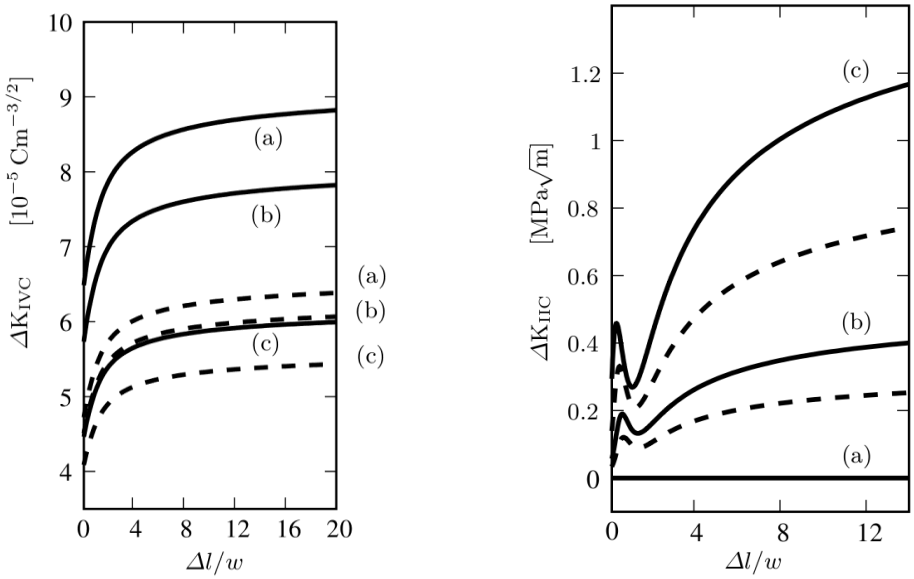

Fig. 3. R-curves for mode-IV (left) and mode-II (right) intensity factors of PZT-5H with poling (left) perpendicular and (right) parallel to the crack faces and combined electromechanical loading. The electrical loads are: (a) $K_{IV}^{\infty} = 0 \cdot K_{IV}^{C}$, (b) $K_{IV}^{\infty} = 0.1 \cdot K_{IV}^{C}$ and (c) $K_{IV}^{\infty} = 0.3 \cdot K_{IV}^{C}$.

The plots show the effective mode-I fracture toughness as a function of the normalized crack extension for an electromechanical loading perpendicular to the crack faces. The electrical loads are given in terms of $K_{IV}^{C} = \sqrt{\pi a} \cdot \kappa E_C$ for demonstration purpose, with E_C being the coercive field and κ the corresponding dielectric constant of the material. As shown in Eq. (4) we consider on the micro-scale three different switching variants which results in three contributions to the effective fracture toughness,

$$\Delta K_L = \Delta K_L^{+90^\circ} + \Delta K_L^{-90^\circ} + \Delta K_L^{180^\circ} . \qquad (6)$$

As expected, electrical loads increase the fracture toughness for both poling directions x_1 and x_2. Further, on the macro-scale two different crack models are analyzed: the solid curves represent the impermeable model with $K_L^{app} = K_L^{\infty}$ and the dashed curves represent the semi-permeable model with $K_L^{app} = K_L^{\infty} - K_L^{C}$, where K_L^{∞} are the external loads and K_L^{C} represent electrostaticaly induced crack surface tractions, see [1,2].

For small electrical loads both models produce similar results. However, the difference becomes larger with increasing electrical loads. It is obvious that the reason for this is due to the different effective loads K_L^{app}. For poling perpendicular to the crack faces applying the semi-permeable crack model results in larger toughness than for the impermeable crack model. In contrast, for poling parallel to the crack faces the effect is opposite. In this case the toughness is lowered by a significant amount.

Summary

In the present work we calculated the R-curves of ferroelectric materials such as PZT-5H considering effects on microscopic and macroscopic length scales, the full anisotropy of the material and the piezoelectric weight functions. On the macro-scale we applied two different crack models: impermeable and semi-permeable. As expected, the fracture toughness is strongly modified by the switching phenomena. Further, the electrical loads play an essential role in toughness variation. The toughness increases with increasing electrical loads for both poling directions. The difference between the impermeable and semi-permeable crack models varies with electrical loads and poling directions. In conclusion, one can state that an electrical field shields the crack tip which increases the fracture toughness with increasing field strength.

References

[1] R. Gellmann and A. Ricoeur: published online by Arch. Appl. Mech. (2011)
[2] R. Gellmann and A. Ricoeur: Proc. Appl. Math. Mech. Vol. 11 (2011), p. 469-470
[3] R. McMeeking and A. Ricoeur: Int. J. Solids Struct. Vol. 40 (2003), p. 6143-6162
[4] T. Zhu and W. Yang: Acta Mater. Vol. 45 (1997), p. 4695-4702
[5] A. Ricoeur and M. Kuna: Computat. Mater. Sci. Vol. 27 (2003), p. 235-249
[6] R.K.N.D. Rajapakse and X. Zeng: Acta Mater. Vol. 49 (2001), p. 877-885
[7] L. Ma: Int. J. Solids Struct. Vol. 47 (2010), p. 3214-3220
[8] A. Ricoeur and M. Kuna: Int. J. Fract. Vol. 157 (2009), p. 3-12
[9] M.J. Busche and K.J. Hsia: Scripta Mater. Vol. 44 (2001), p. 207-212
[10] Y. Yamashita, S. Sakakibara, H. Yamamoto, Y. Sakabe and G.J. Pezzotti: J. Appl. Phys. Vol. 98 (2005), p. 034110
[11] F. Fang, W. Yang, F.C. Zhang and H.S. Luo: J. Am. Ceram. Soc. Vol. 88 (2005), p. 2491-2497

[12] D. Fang, Y. Jiang, S. Li and C.T. Sun: Acta Mater. Vol. 55 (2007), p. 5758-5767
[13] S.C. Hwang, J.E. Huber, R.M. McMeeking and N.A. Fleck: J. Appl. Phys. Vol. 84 (1998), p. 1530-1540
[14] X. Chen, D.N. Fang and K.C. Hwang: Acta Mater. Vol. 47 (1997), p. 3181-3189
[15] Y.Z. Huo and Q. Jiang: Int. J. Solids Struct. Vol. 35 (1998), p. 1339-1353
[16] W. Lu, D.N. Fang and K.C. Hwang: Acta Mater. Vol. 47 (1999), p. 2913-2926
[17] J.E. Huber, N.A. Fleck, C.M. Landis and R.M. McMeeking: J. Mech. Phys. Solids Vol. 47 (1999), p. 1663-1697
[18] J. Li and G.J. Weng: Proc. R. Soc. London A, Vol. 455 (1999), p. 3493-3511
[19] T. Steinkopff: J. Eur. Ceram. Soc. Vol. 19 (1999), p. 1247-1249
[20] J.E. Huber and N.A. Fleck: J. Mech. Phys. Solids Vol. 49 (2001), p. 785-811
[21] Y. Su and G.J. Weng: Proc. R. Soc. London A, Vol. 462 (2006), p. 1763-1789
[22] S.C. Hwang, C.S. Lynch and R.M. McMeeking: Acta Metall. Mater. Vol. 43 (1995), p. 2073-2084